Supporting Information

Anthracene Derivatives with Strong Spin-Orbit Coupling and Efficient High-Lying Reverse Intersystem Crossing Beyond the El-Sayed Rule

Ki Ju Kim[1], Jaesung Kim[1], Jong Tae Lim[2], Jinyeong Heo[3], Bum Jun Park[1], Hyewon Nam[1], Hyeonwoo Choi[4], Seung Soo Yoon[3], Woojae Kim[4*], Sunwoo Kang[5*], Taekyung Kim[1,6*]

[1]Department of Information Display, Hongik University, Seoul 04066, Republic of Korea
[2]Research on core technology convergence of metamaterials, Hongik University, Seoul 04066, Republic of Korea`
[3]Department of Chemistry, Sungkyunkwan University, Suwon 16419, Republic of Korea
[4]Department of Chemistry, Yonsei University, Seoul 03722, Republic of Korea
[5]Display Research Center, Samsung Display Co., Yongin, Republic of Korea, 17113
[6]Department of Materials Science and Engineering, Hongik University, Sejong, 30016, Republic of Korea

EXPERIMENTS

Synthesis

All reagents and solvents were used without purification and obtained from a commercial supplier (Sigma-Aldrich or TCI). ^{1}H nuclear magnetic resonance (NMR) spectra were recorded on a Bruker Avance III 500 MHz NMR spectrometer, using $CDCl_3$ as the solvent at 298 K. Tetramethylsilane (TMS) was used for ^{1}H NMR as internal standards. 2MIQ-NPA was synthesized by the Pd-catalyzed Suzuki-Miyaura coupling reaction.

In a 250 ml, two-necked, round-bottomed flask fitted with an efficient stirrer, dropping funnel, and reflux condenser has placed a mixture of 2.33 g (5.50 mmol, 1.10 eq) of (10-(4-(naphthalen-1-yl)phenyl)anthracene-9-yl)boronic acid, 1.62 g (5.00 mmol, 1.00 eq) of 9-bromo-7,7-dimethyl-7H-indeno[1,2-f]quinoline, 0.23 g (0.22 mmol, 0.04 eq) of tetrakis(triphenylphosphine)palladium(0) ($Pd(PPh_3)_4$), and 65 ml of toluene. And then, the slurry solution is heated to 100^{o}C and stirred, while a solution (3M) of 5.30 g (50.0 mmol, 10.0 eq) of sodium carbonate in 17.0 ml of water and 6 ml of ethanol is added through a dropping funnel. After refluxing for 3 hours with a violent stir, the slurry solution turns pale orange to dark blue. The crude product was extracted with methylene chloride, washed with aqueous sodium chloride, and dried with magnesium sulfate. After filtration and evaporation of the solvent, the crude product was purified by column chromatography (silica gel, ethyl acetate:hexane= 1:4) and washing with methyl alcohol to give the desired compound of 2MIQ-NPA as a white solid (1.46 g, 46.9%). ^{1}H-NMR (500 MHz, $CDCl_3$) δ 9.19 (d, *J*= 8.4 Hz, 1H), 9.02 (dd, *J*= 4.1, 1.5 Hz, 1H), 8.49 (d, *J*= 7.9 Hz, 1H), 8.20 (dd, *J*= 9.2, 3.1 Hz, 2H), 8.02-7.97 (m, 1H), 7.97-7.89 (m, 4H), 7.89-7.83 (m, 2H), 7.77 (d, *J*= 8.0 Hz, 2H), 7.72 (d, *J*=1.5 Hz, 1H), 7.68-7.54 (m, 8H), 7.48-7.37 (m, 4H), 1.66 (s, 6H).

Measurements

The differential pulse voltammetry (DPV) was carried out using electrochemical analyzer (PGSTAT101, E-Chem Technology) to obtain HOMO and LUMO. The organic molecules were resolved in N_2 purged-DMF solvent with 0.1 M tetrabutylammonium hexafluorophosphate ($TBAPF_6$) as the supporting electrolyte. The differential pulse condition is as follows 0.2 s pulse width, 0.5 s period, 25 mV step height. Ferrocenium-ferrocene (Fc+/Fc) was used as standard material. The HOMO and LUMO were determined by the formula HOMO/LUMO (eV) = 4.8 – Fc+/Fc potential + first oxidation/reduction potential.

The UV-vis absorption and PL spectra were measured at room temperature using UV-Visible spectroscopy (Agilent 8453) and fluorescence spectrometer (FS5, Edinburgh instruments). The samples were prepared at a concentration of 10 μM in order to prevent inert filter effect.

The transient PL spectra were recorded by fluorescence spectrometer (FS5) equipped with time-correlated single-photon counting (TCSPC; 1024 channel) mode. Excitation for TCSPC was provided by a 375 nm pulsed laser.

Nanosecond transient absorption (ns-TA) spectroscopy was studied using a commercial pump-probe system (EOS, Ultrafst Systems), having ~800 ps time resolution. For the excitation pulse, the 1 kHz repetition rate femtosecond pulses obtained from the optical parametric amplifier was used. The white light supercontinuum probe (360–1600 nm, with spectral resolution of 1.5 nm (VIS) and 3.5 nm (NIR)) was generated by focusing a Nd:YAG laser pulse into a photonic crystal fiber. The probe pulses were electronically synchronized with the femtosecond regenerative amplifier, and the pump-probe delay time was controlled by a digital delay generator (CNT-90, Pendulum Instruments). To minimize the noise, the probe beam was referenced with respect to the signal channel. all the 2MIQ-NPA and PtOEP samples were prepared at 10^{-3} M and 10^{-4} M respectively, and purged with Ar for 15 min before

measurements and encapsulated with cap during measurements.

The *J—V—L* characteristics and the EL spectra were measured using a Keithley Series 2400 source meter and a CS-1000 A (Minolta) spectrometer at an applied voltage. Impedance analyzer (Alpha-AN, Novocontrol) were used to obtain capacitance data at 1kH frequency and 50 mV AC bias.

To measure the transient EL spectra, a function pulse generator (Agilent 33612A) with rise/falling time of 4 ns and 1 kHz pulse voltage was used to drive the devices. The EL signals were detected by a fast photo multiplier tube (HAMAMATSU H10492), and captured for analysis by a Oscilloscope (Agilent DSOX 1102G). The applied pulse period and width were 1 ms and 500 μs.

For mageto-electroluminescence (MEL) measurements, magnetic field was applied with permanent magnet pair moving on the rail. Voltage was applied using a source meter (Keithley 2400), and light intensity was detected by photomultiplier tube (Hamamatsu, H13661) and collected as EL data using a multimeter (Keysight, 34465a). The OLED devices were mounted between two magnets and the magets moved twoard the device at a speed of 10 mm/s through motor motion to a point where the central magnetic field reaches a maximum of 300 mT. The magnetic field at the center of the device was pre-calibrated as a function of the distance between the magnets. The MEL data were obtained according to the formula as follows

$$MEL = \frac{I(B) - I(B_0)}{I(B_0)}$$

where I(B) and I(B_0) represents the EL intensity when magnetic field was applied and not applied.

OLED fabrication

Indium tin oxide (ITO) coated glass with sheet resistance of 30 Ω /sq and thickness of 150 nm were cleaned in ultrasonic baths (acetone, , distilled water, and isopropyl alcohol) for 15 min each. Before depositing organic layers, pre-cleaned ITO-coated glass substrates were dried in a convection oven at 120 ℃ for 10 min. After then, the ITO/glass substrates were treated with O_2 plasma at 2×10-2 Torr and 150 W condition for 2 min. Organic layers were deposited by thermal evaporator with shadow mask under high vacuum (2×10^{-7} Torr) condition. Aluminum (Al) cathode was deposited at a rate of 1.5 Å/s. The deposition rates were controlled with a quartz crystal monitor. In encapsulation process, glass cap and UV-epoxy resin were used to prevent degradation from ambient condition. The getter was attached under the glass cap to absorb the residue moisture in the encapsulated device, which has an active layer of 2×2 mm^2.

Non-doped device structure: indium tin oxide (ITO)/NDP-9 3 wt.% doped BCFN (10 nm)/BCFN (60 nm)/BPADBF (5 nm)/EML (20 nm)/ SFXBPTrz (5 nm)/DNPQTrz (30 nm)/Liq (1.5 nm)/Al (100 nm), where 2-(7-dicyanomethylene-1,3,4,5,6,8,9,10-octafluoro-7H-pyrene-2-ylidene)-malononitrile (NDP-9), N-([1,1'-biphenyl]-4-yl)-9,9-dimethyl-N-(4-(9-phenyl-9H-carbazol-3-yl)phenyl)-9H-fluoren-2-amine (BCFN), N-([1,1'-biphenyl]-4-yl)-N-(4-(dibenzo[b,d]furan-2-yl)phenyl)dibenzo[b,d]furan-3-amine (BPADBF), 2,4-diphenyl-6-(3'-(spiro[fluorene-9,9'-xanthen]-2-yl)-[1,1'-biphenyl]-3-yl)-1,3,5-triazine (SFXBPTrz), 8-(4-(4,6-di(naphthalen-2-yl)-1,3,5-triazin-2-yl)phenyl)quinoline (DNPQTrz), 8-hydroxyquinolinolato lithium (Liq) as the p-dopant, hole-transporting, electron-blocking, hole-blocking, electron-transporting, and electron-injection layers, respectively.

TTF absent device structure: HAT-CN (10 nm)/TAPC (50 nm)/TCTA (10 nm)/mCBP (5 nm)/mCBP: Ref or 2MIQ-NPA 1 wt.% (20 nm)/mSiTrz (5 nm)/TPBi (30 nm)/Liq (1.5 nm)/Al (100 nm), where HAT-CN is 1,4,5,8,9,11-hexaazatriphenylenehexacarbonitrile, TAPC is di-

(4-(N,N-ditolyl-amino)-phenyl)cyclohexane, TCTA is tris(4-carbazoyl-9-ylphenyl)amine, mCBP is 3,3-di(9H-carbazol-9-yl)biphenyl, mSiTrz is 2-phenyl-4,6-bis(3-(triphenylsilyl)phenyl)-1,3,5-triazine, and TPBi is 2,2',2''-(1,3,5-benzinetriyl)-tris(1-phenyl-1-H-benzimidazole).

Calculation of f_{DF} from transient EL data

Given the approximation that there is no triplet-polaron quenching process and the rate constant of TTA (k_{TT}) is constant, $\frac{dN_T}{dt} = -k_{nr}N_T - k_{TT}N_T^2$, where N_T is triplet density at a time of t and k_{nr} is non-radiative rate constant. when $k_{nr} << k_{TT}$, the solution to N_T is as follows. $N_T = \frac{1}{k_{TT} \cdot t + C}$, where C equals $\frac{1}{N_T(0)}$. Because the TTF is bimolecular quenching process, the EL intensity of delayed fluorescence (I_{DF}) can be expressed as $I_{DF} \propto N_T^2$. f_{DF} values were extracted from the y-intercept of following Equation.

$$\frac{1}{\sqrt{I_d}} \propto \frac{1}{N_T(0)} + k_{TT}t$$

Numerical simulation of transient EL data

To simulate the transient EL data, the polaron dynamics were considered recombined polaron density and accumulated polaron density in the equilibrium state with the ratio of α and $(1 - \alpha)$[1]. The time-dependent polaron, singlet, and triplet density are expressed with following equations.

at $t < t_0$, where t_0 is turn-off time.

$$\frac{dn_{rec}}{dt} = (1-\alpha)\left(\frac{j}{ed} - \gamma n_{t_0 t}^2\right) \tag{1}$$

$$\frac{dn_{acc}}{dt} = \alpha\left(\frac{j}{ed} - \gamma n_{tot}^2\right) \tag{2}$$

$$\frac{dS_1}{dt} = P_s \gamma n_{rec}^2 - (k_r + k_{nr})S_1 + \frac{1}{2} f k_{TT} T_{1+}^2 + k_{hrisc}' T_1 \tag{3}$$

$$\frac{dT_1}{dt} = (1-P_s)\gamma n_{rec}^2 - k_T T_1 - k_{TT} T_1^2 - k_{hrisc}' T_1 \tag{4}$$

at $t > t_0$

$$n_{acc}(t) = \frac{\alpha}{2\tau} exp^{\frac{1}{2\tau}\left(2\mu + \frac{\sigma^2}{\tau} - 2t\right)} erfc\left(\frac{\mu + \frac{\sigma^2}{\tau} - t}{\sqrt{2}\sigma}\right) n_{acc}(t_0) \tag{5}$$

$$\frac{dS_1}{dt} = P_s \gamma n_{acc}^2 - (k_r + k_{nr})S_1 + \frac{1}{2} f k_{TT} T_{1+}^2 + k_{hrisc}' T_1 \tag{6}$$

$$\frac{dT_1}{dt} = (1-P_s)\gamma n_{acc}^2 - k_T T_1 - k_{TT} T_1^2 - k_{hrisc}' T_1 \tag{7}$$

$$P_s = \eta_{PF}/100 \tag{8}$$

$$f = \frac{I_{DF}(1-P_s)}{2 I_{pF} P_s} \tag{9}$$

$$\gamma = \frac{q(\mu_e + \mu_h)}{\varepsilon_0 \varepsilon_r} \tag{10}$$

j,*e* and *d* is current density, elementary charge and thickness of EML respectively. γ is Langevin recombination coefficient. n_{rec} and n_{acc} are the polaron densities that involves in the recombination and

accumulation. The modified Gaussian distribution function concerning relaxation of accumuulated polarons was used to fit the initial region after pulse off. τ, μ and σ are the time of an exponential component, mean value, and variance of the Gaussian component. k_r and k_{nr} are the radiative and non-radiative rate constant of S_1. k_{TT} and k_T are bimolecular quenching rate constant of T_1 and the non-radiative rate constant of T_1, respectively. f is the probability of spin-restrict statistic of two triplets to one singlet. This value can be derived from equation (9) referred by [2]. P_s is the ratio of promptly generated singlets including direct hRISC process from T_n to S_1. To describe the exact exciton dynamics including TTF and TTF-mediated-hRISC, the concentration change rate of intermediate states such as T_n, ^{1}(TT), and ^{3}(TT) should be included. However, the more complex dynamic processes is included, the lower accuracy and credibility simulation would be acquired. Therefore, to simplify the TTF-mediated-hRISC process, the new rate constant, $k_{hrisc}^{'}$ is introduced in assumption with that T_n density generated from TTF-mediated-hRISC is proportional to T_1 density. The k_{TT}, k_T and $k_{hrisc}^{'}$ were set to be fitting parameters.

At 5V, the current density (j) of Ref and 2MIQ-NPA device are 42, 61.3 mA/cm^2

Reference

1. K. H. Lee, S. O. Jeon, Y. S. Chung, J. M. Kim and J. Y. Lee, *Advanced Optical Materials*, 2023, **11**, 2201687.
2. S. Xiao, X. Qiao, C. Lin, L. Chen, R. Guo, P. Lu, L. Wang and D. Ma, *Advanced Optical Materials*, 2022, **10**, 2102333.

(a)

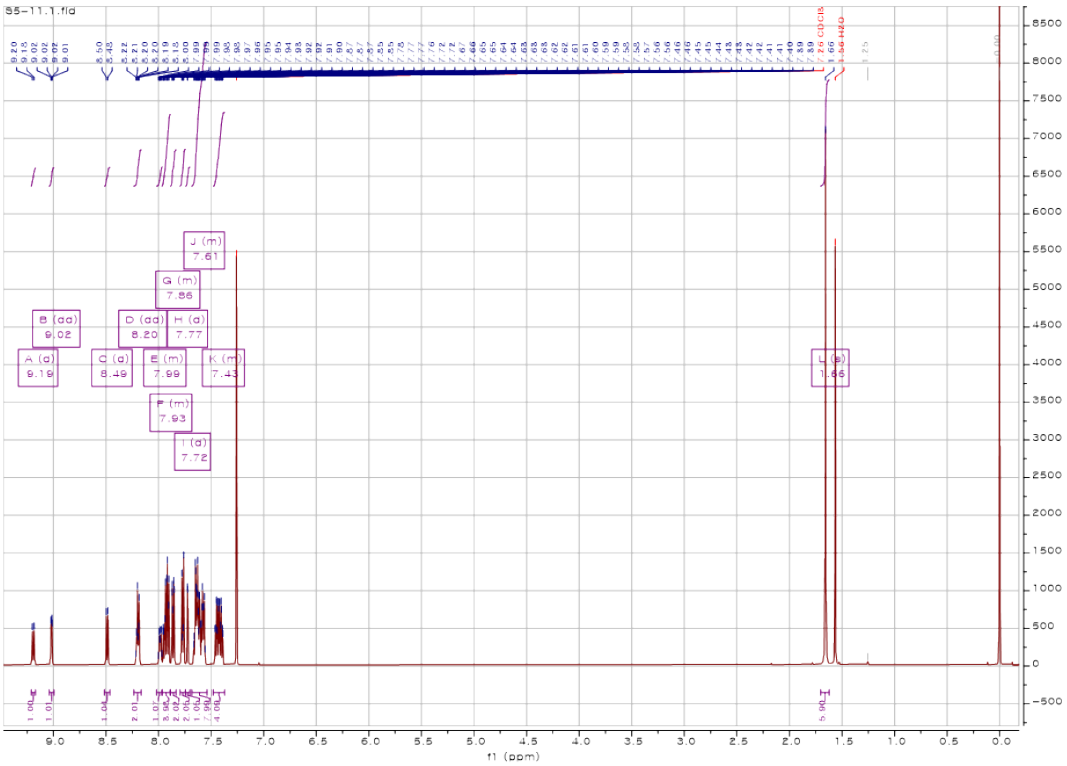

(b)

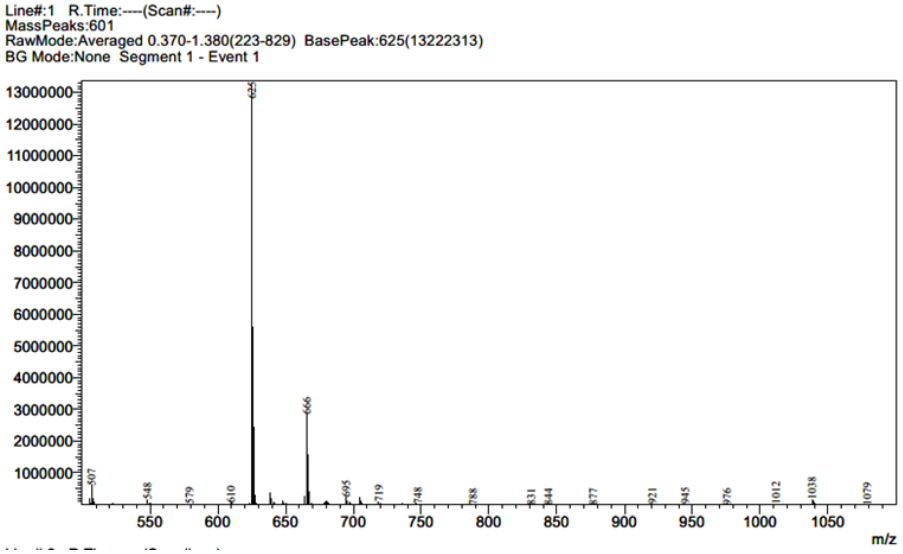

Fig. S1. (a) ^{1}H NMR and (b) mass spectrum of 2MIQ-NPA.

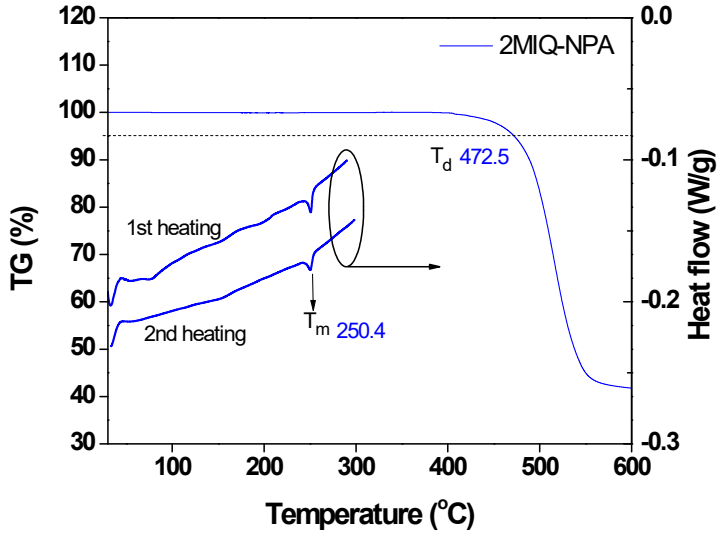

Fig. S2. TGA and DSC data of 2MIQ-NPA.

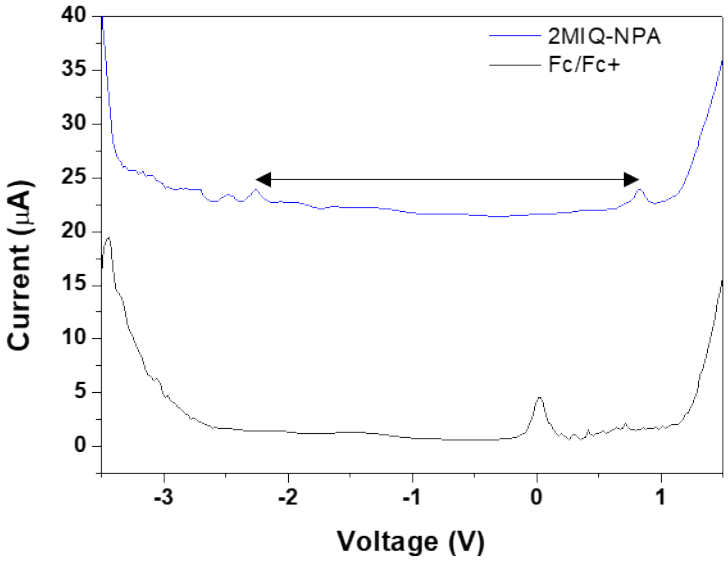

Fig. S3. Differential pulse voltammetry results of 2MIQ-NPA in DMF solvent with 0.1 M $TBAHFP_6$ electrolyte. The oxidation peak of Fc/Fc+ is 0.03 V.

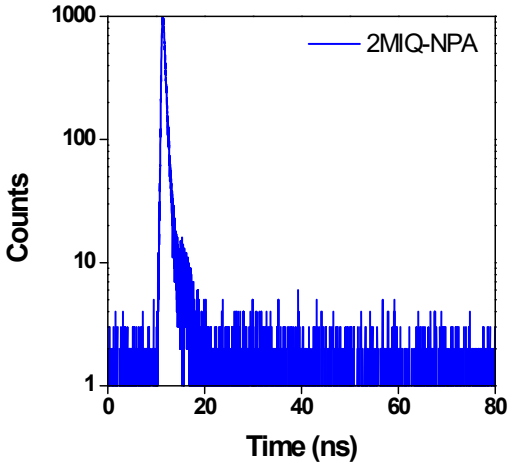

Fig. S4. Transient PL spectra of 2MIQ-NPA in neat film.

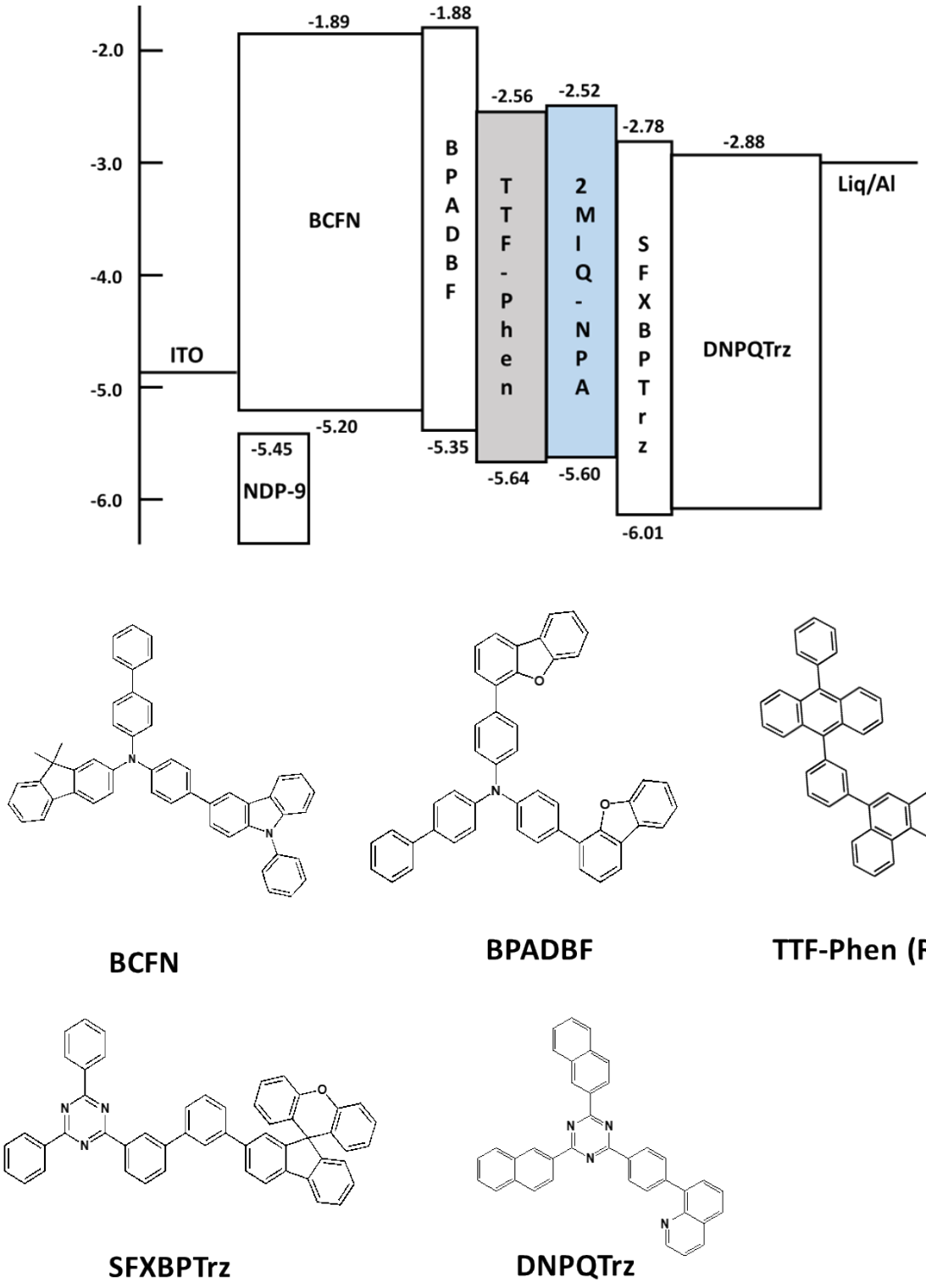

Fig. S5. (Top) The energy level alignment of materials used in non-doped devices and (bottom) molecular structures of common layers.

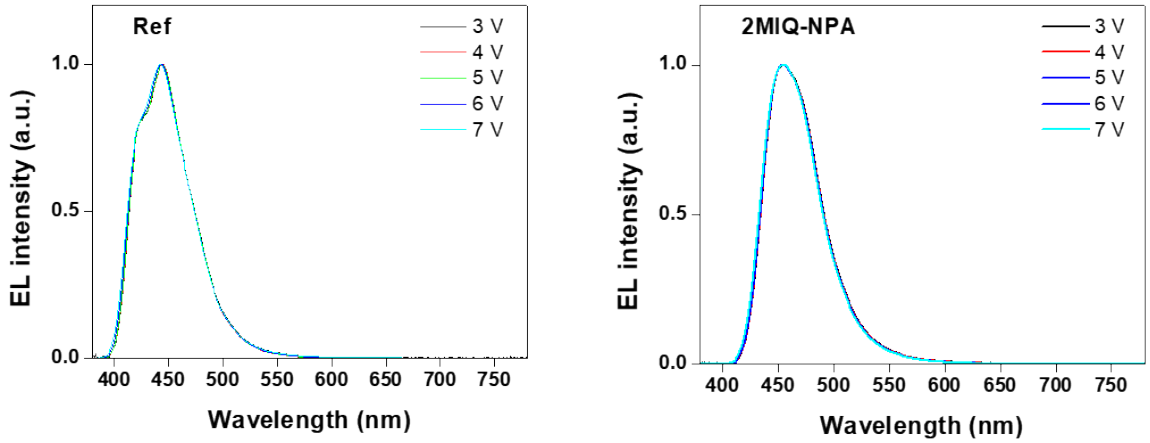

Fig. S6. Voltage dependent EL spectra of non-doped devices.

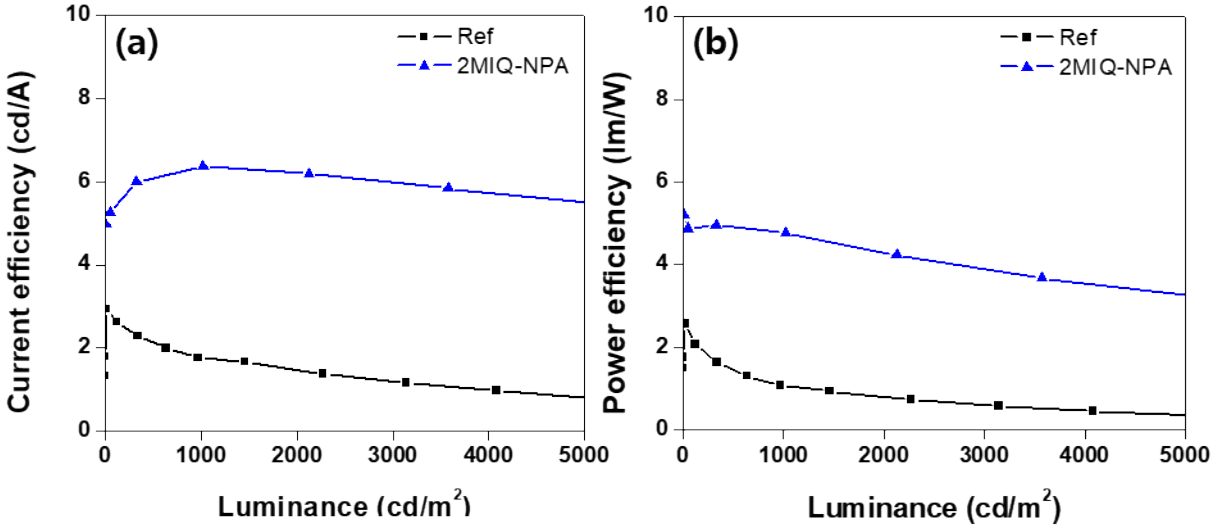

Fig. S7. (a) Current efficiency-luminance and (b) power efficiency-luminance characteristics of non-doped devices.

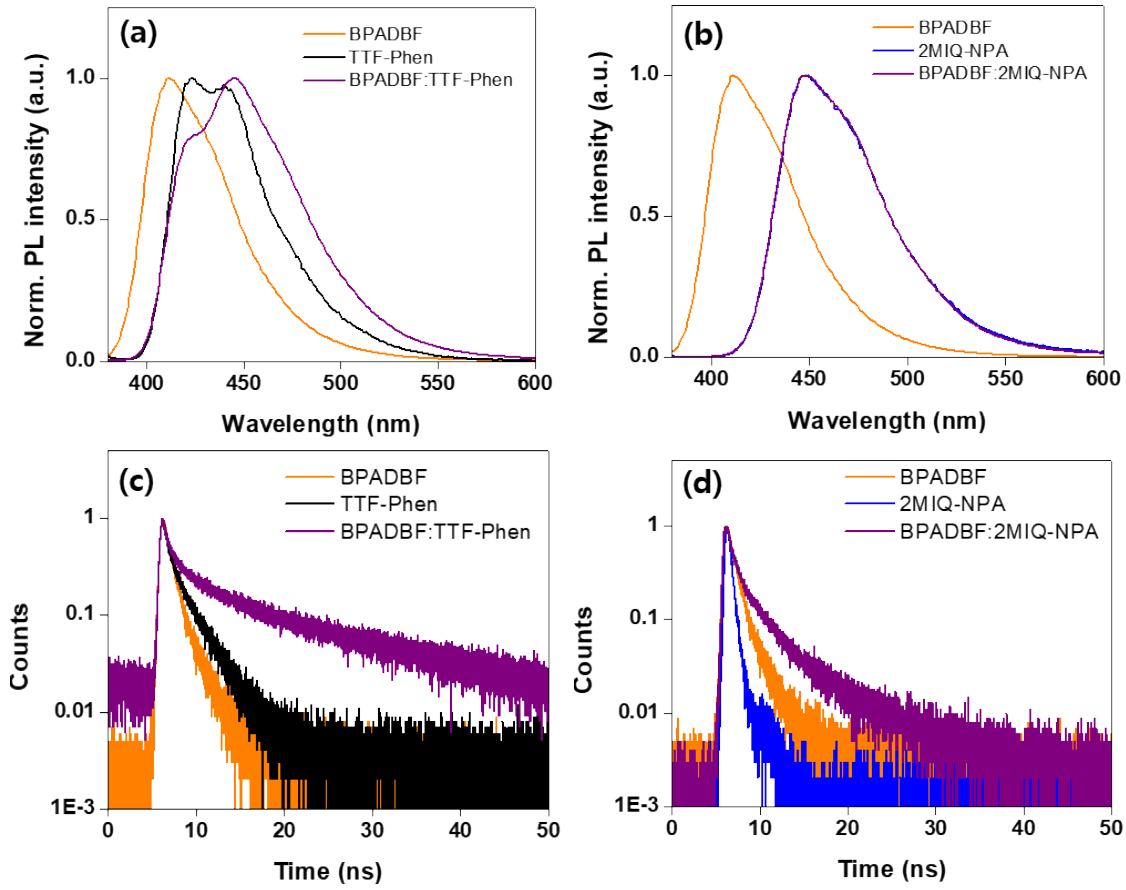

Fig. S8. (a), (b): film PL spectra and (c), (d): transient PL spectra of TTF-Phen and 2MIQ-NPA with BPADBF.

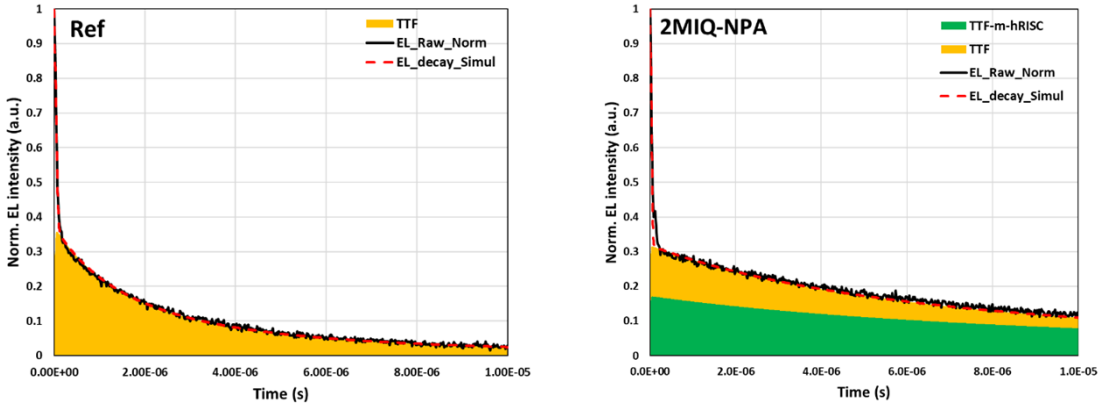

Fig. S9. The simulated results of Ref and 2MIQ-NPA devices at 5V. The colored area indicates the contribution to delayed fluorescence by TTF (yellow) and TTF-mediated hRISC (green).

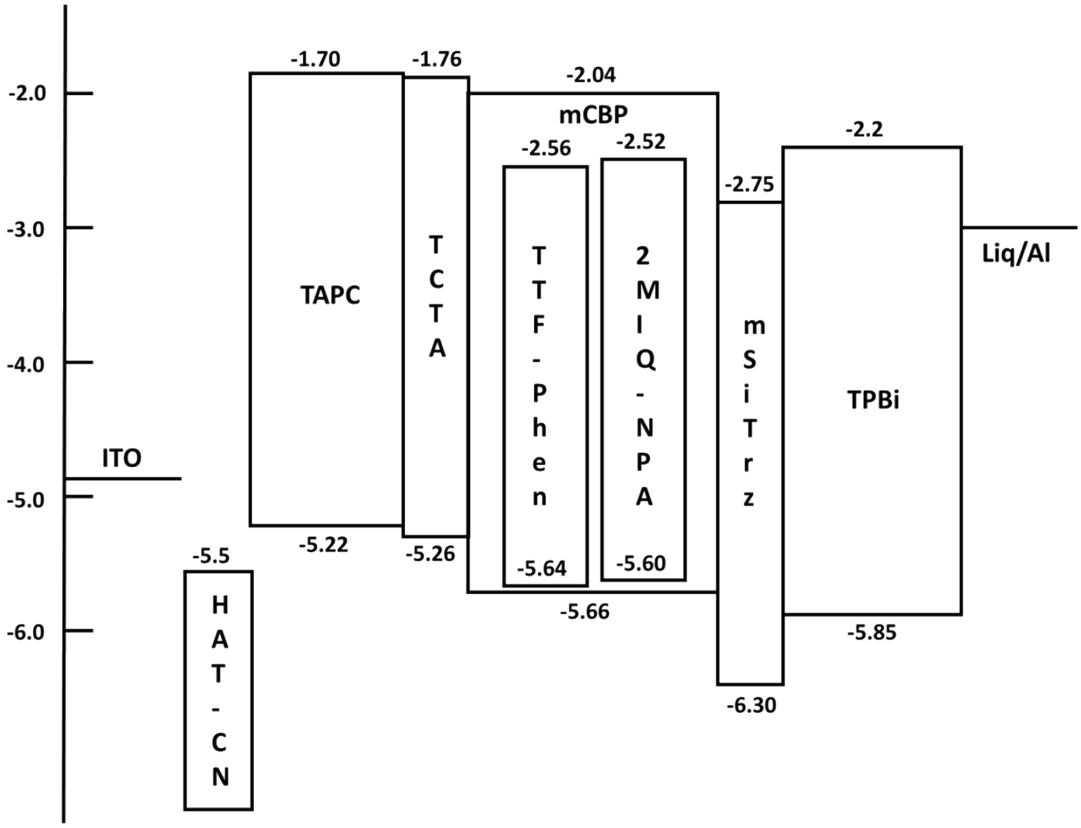

Fig. S10. The energy level alignment of materials used in TTF absent devices.

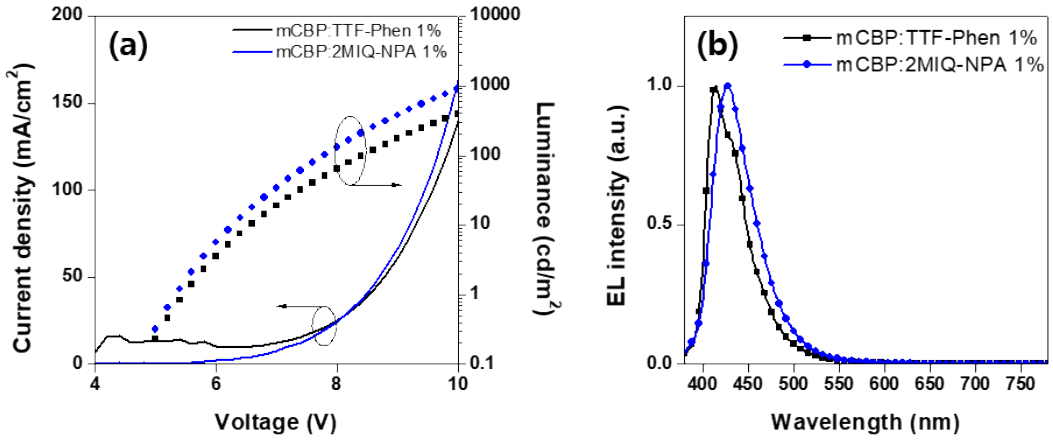

Fig. S11. (a) Current density-voltage-luminance characteristics and (b) EL spectra of TTF absent devices.

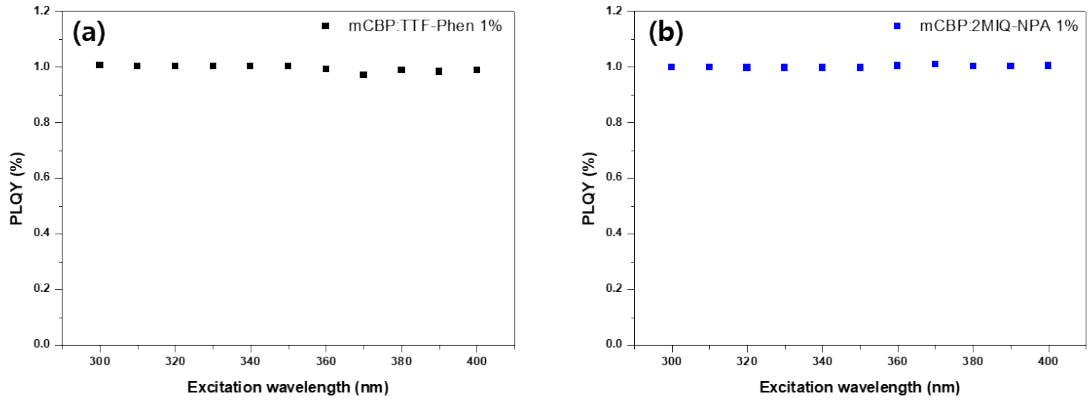

Fig. S12. PLQY data according to excitation wavelength of (a) mCBP:TTF-Phen 1% doped film and (b) mCBP:2MIQ-NPA 1% doped film.

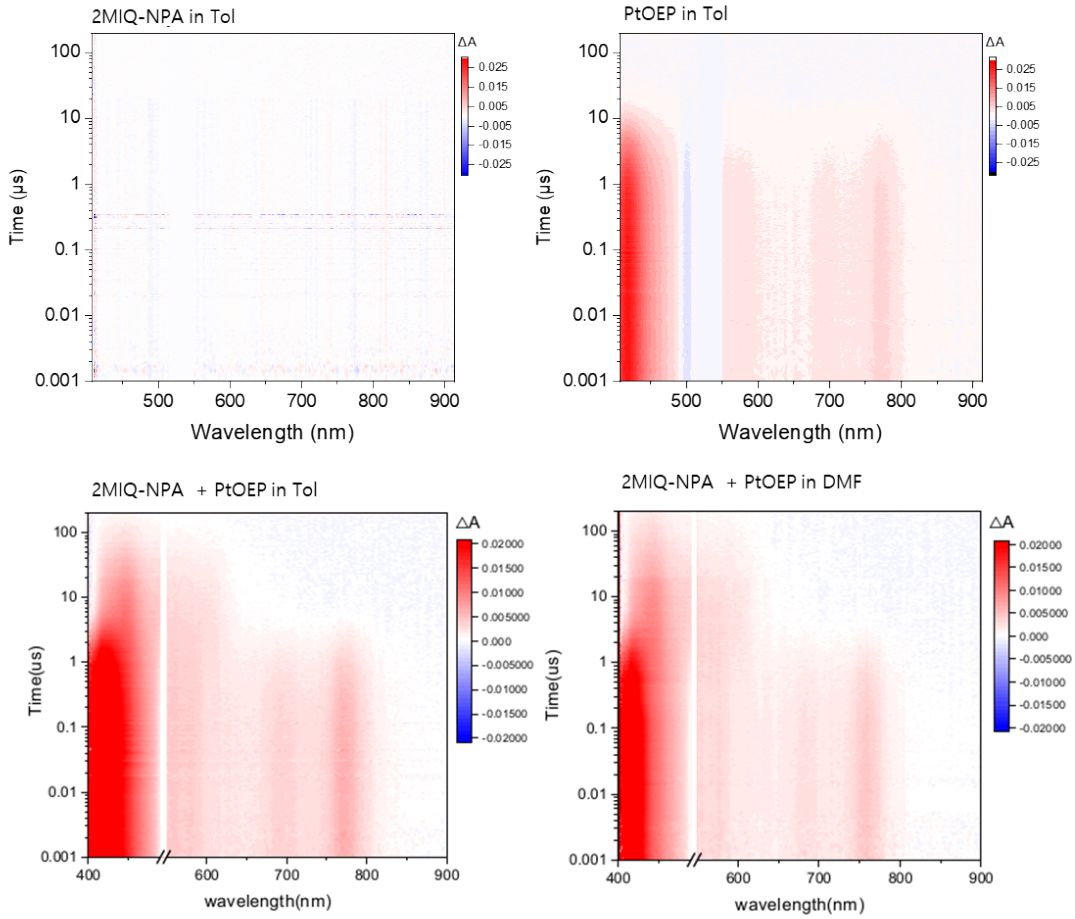

Fig. S13. ns-TA 2D contour map of (a) 2MIQ-NPA in toluene, (b) PtOEP in toluene and 2MIQ-NPA & PtOEP in (c) toluene and (d) DMF.

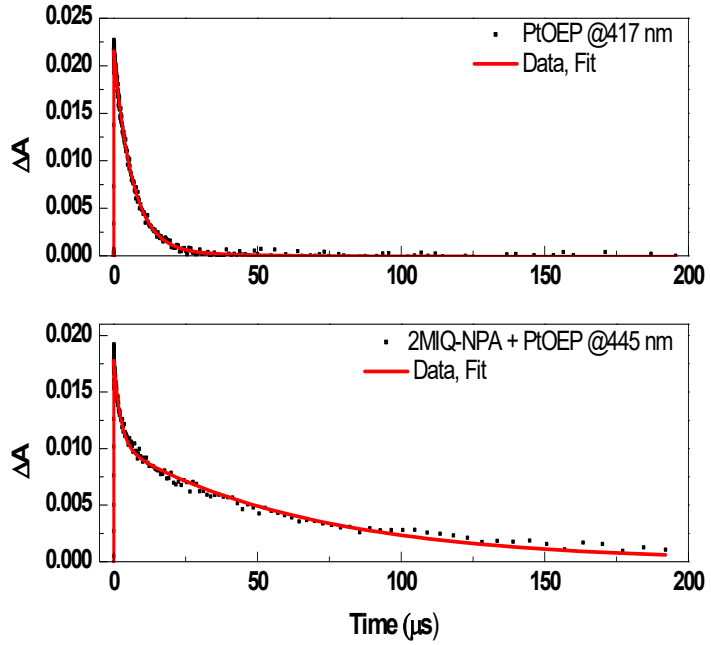

Fig. S14. Transient absorption decay of PtOEP (up) and 2MIQ-NPA and PtOEP (down) in toluene solution probed at 417 and 445 nm wavelength.

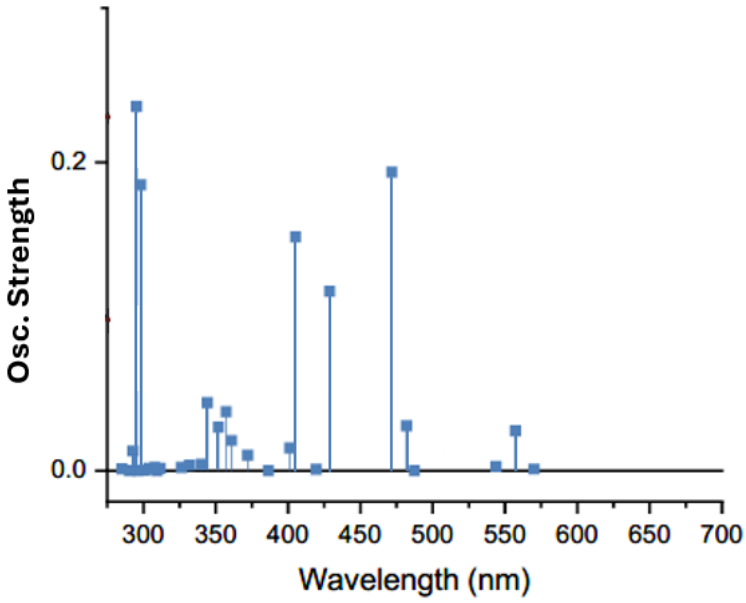

Fig. S15. Oscillator strength from T_1 to T_n state transition of 2MIQ-NPA. The TD-DFT calculation was carried out after geometry optimization of T_1 state using M062X/6-31g(d) functional/basis set.

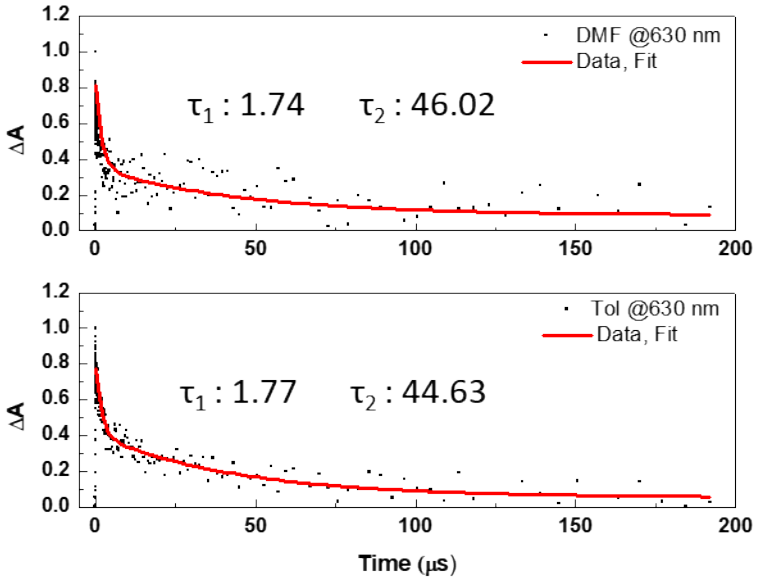

Fig. S16. Transient absorption decay probed at 630 nm of 2MIQ-NPA and PtOEP in DMF (up) and toluene (down).

Table S1. The device performances of non-doped and TTF absent device.

Device	V_{on}	L_{max}	CE_{max}	PE_{max}	EQE_{max}	EQE_{1000}	CIE_x	CIE_y	λ_{EL}
Ref	3.03	5646	2.86	2.65	5.57	3.78	0.15	0.05	442
2MIQ-NPA	2.87	14230	6.37	5.27	7.01	6.77	0.14	0.11	454
mCBP: TTF-Phen 1%	5.46	678	0.28	0.10	0.85	-	0.16	0.04	414
mCBP: 2MIQ-NPA 1%	5.33	1383	0.57	0.21	1.32	1.29	0.16	0.05	428

Table S2. The results of numerical simulation for transient EL data at 5V

Device	P_s	f	α ($\times 10^{-4}$)	γ ($\times 10^{-12}$)	τ	σ	μ	k_{TT} ($\times 10^{-13}$)	$k_{hrisc}^{'}$ ($\times 10^{4}$)	k_T ($\times 10^{3}$)
Ref	0.23	0.358	3.3	4.93	0.003	0.5	0.04	7	-	1

2MIQ-NPA	0.44	0.719	2.8	4.07	0.003	0.34	0.04	1	3	0.1